Contents lists available at ScienceDirect

Digital Chinese Medicine

journal homepage: http://www.keaipublishing.com/dcmed

# Mechanism of Bugansan Decoction in ameliorating learning and memory impairment in D-galactose-induced aging rats based on AGEs/RAGE/NF-κB pathway

LI Wei[a], WANG Shuo[a], WANG Jiepeng[a, b], FANG Fang[a, b], FANG Chaoyi[a, b*]

*a. School of Preclinical Medicine, Hebei University of Chinese Medicine, Shijiazhuang, Hebei 050200, China*

*b. Hebei Key Laboratory of Integrated Chinese and Western Medicine for Lung Disease Research, Shijiazhuang, Hebei 050091, China*

ARTICLE INFO

*Article history*
Received 04 August 2023
Accepted 13 September 2023
Available online 25 September 2023

*Keywords*
Bugansan Decoction (补肝散, BGSD)
Liver Qi deficiency
Aging
Learning and memory
Neuroinflammation
AGEs/RAGE/NF-κB signaling pathway

ABSTRACT

**Objective** To investigate the underlying mechanism of the compound Bugansan Decoction (补肝散, BGSD) in intervening learning and memory in D-galactose (D-gal)-induced aging rats.

**Methods** A total of 40 rats were randomly assigned to four groups: control, model, BGSD [14.06 g/(kg·d)], and piracetam [0.4 g/(kg·d)] groups, with 10 rats in each group. D-gal [400 mg/(kg·d)] was injected intraperitoneally to establish the aging rat model. The rats' body weight, water intake, food intake, and gripping strength were recorded each week. The eight-arm maze and step-down test were used to measure the rats' capacity for learning and memory. Liver, thymus, spleen, and brain tissues were weighed to calculate the corresponding organ indices; serum malondialdehyde (MDA) content and superoxide dismutase (SOD) activity were measured. Hematoxylin and eosin (HE) staining was adopted to observe the pathological changes of the hippocampus; enzyme-linked immunosorbent assay (ELISA) was used to detect the levels of tumor necrosis factor (TNF)-$\alpha$, interleukin (IL)-6, and IL-1$\beta$ in the hippocampus. Real-time quantitative polymerase chain reaction (RT-qPCR) was used to detect the expression of receptors for advanced glycation end products (RAGE), nuclear factor-κB (NF-κB), TNF-$\alpha$, IL-6, and IL-1$\beta$ mRNA in the hippocampus. Western blot (WB) was employed to detect the expression levels of advanced glycation end products (AGEs), RAGE, and NF-κB protein in the hippocampus.

**Results** In D-gal-induced aging rats, BGSD significantly increased food intake, water intake, body weight, gripping strength, and organ indices ($P < 0.05$), and significantly decreased working memory error (WME), reference memory error (RME), and total memory errors (TE) in an eight-arm maze ($P < 0.05$). In the step-down test, step-down latency was prolonged and the frequency of errors dropped ($P < 0.05$). Additionally, BGSD could lessen the harm done to hippocampus neurons, increase serum SOD activity, lower MDA levels, and down-regulate the expression levels of the pro-inflammatory molecules TNF-$\alpha$, IL-6, and IL-1$\beta$ ($P < 0.05$). Further findings showed that BGSD significantly decreased hippocampal AGEs, RAGE, and NF-κB expression ($P < 0.05$).

**Conclusion** By blocking the AGEs/RAGE/NF-κB signaling pathway, BGSD may regulate the neuroinflammatory damage in D-gal-induced aging rats, and thus improve learning and memory.

*Corresponding author: FANG Chaoyi, E-mail: hbfcy@163.com.

Peer review under the responsibility of Hunan University of Chinese Medicine.

DOI: 10.1016/j.dcmed.2023.10.007

**Citation:** LI W, WANG S, WANG JP, et al. Mechanism of Bugansan Decoction in ameliorating learning and memory impairment in D-galactose-induced aging rats based on AGEs/RAGE/NF-κB pathway. Digital Chinese Medicine, 2023, 6(3): 317-327.

## 1 Introduction

Aging is a normal and natural physiological process that is inevitably accompanied by tissue and organ breakdown and dysfunction, as well as several serious disorders [1, 2]. Global aging is on the rise, and China has already begun to enter an aging society [3]. Age-related neurodegenerative symptoms, such as memory loss and learning impairment, have progressively appeared in the body and have placed an enormous burden on family and society. Although the molecular mechanism of aging remains mysterious and complicated, inflammatory response, oxidative stress, autophagy, mitochondrial injury, and dysfunction of telomerase are related to aging or aging-related diseases [4]. In previous studies, a positive correlation has also been confirmed between aging and the progressive increase in inflammatory cytokines [5, 6]. A long-term inflammatory reaction is related to the decline of learning and memory in particular [5, 7]. Long-term administration of D-galactose (D-gal) could impair learning and memory, as well as motor skills in animals and the symptoms are similar to aging [8, 9]. Moreover, D-gal-induced aging in rats has been widely used to investigate the mechanisms of aging and observe potential anti-aging agents [8].

As an important part of complementary and alternative therapies, traditional Chinese medicine (TCM) has distinctive perspectives on aging. *Miraculous Pivot · In Natural Life Span* (*Ling Shu · Tian Nian*, 《灵枢·天年》) says: "at the age of 50, the liver Qi begins to decline and the liver lobes begin to thin, the bile begins to disappear, and the eyes begin to be unclear". Therefore, deficiency of liver Qi is the initial factor of aging. Bugansan Decoction (BGSD) is a TCM preparation from *Standards for Diagnosis and Treatment* (*Zheng Zhi Zhun Sheng*, 《证治准绳》) created by HUA Boren in Ming Dynasty and is a representative prescription with the function of tonifying liver Qi. Besides, the main components of BGSD have potential therapeutic effects on aging and aging-related diseases. For example, Huangqi (Astragali Radix) and its active ingredients showed anti-aging effects [10]. Similarly, Shanzhuyu (Corni Fructus), Danggui (Angelicae Sinensis Radix), and their extracts provide neuroprotection and anti-neuroinflammatory activity, improve memory, and prevent aging [11-13]. Based on this, our research group has previously attempted to explore the effect of BGSD on learning and memory impairment in aging rats and revealed its beneficial effects [14], but the potential mechanism remains unclear.

Neuroinflammation is one of the critical factors that could speed up the aging process [7]. Increasing evidence also supports that the binding of advanced glycation end products (AGEs) to receptors of AGEs (RAGE) contributes to the occurrence of neurodegenerative disorders by promoting nuclear factor-$\kappa$B (NF-$\kappa$B) [15, 16]. AGEs/RAGE/NF-$\kappa$B signaling pathway is essential for neuroinflammation [17] and the modulation of learning and memory [18]. However, it is unknown whether the neuroinflammation caused by AGEs/RAGE/NF-$\kappa$B is connected to the intervention of BGSD on learning and memory impairment in aging rats. Therefore, this study aimed to ascertain whether BGSD has a protective effect against learning and memory decline in aged rats and to analyze its molecular mechanism from the viewpoint of the AGEs/RAGE/NF-$\kappa$B signaling pathway. Our research would provide experimental evidence for the further clinical practice of BGSD.

## 2 Materials and methods

### 2.1 Animals

Forty male Sprague-Dawley (SD) rats (6 - 8 weeks, body weight: 160 - 200 g) in specific-pathogen-free (SPF) grade were purchased from Beijing Vital River Laboratory Animal Technology Co., Ltd. (SCXK [Jing] 2016-0006). The rats were housed in a room with standard laboratory conditions (temperature, 20 - 25 °C; humidity, 30% - 40%; a 12 h light/dark cycle) and allowed access to water and food ad libitum. All the experimental protocols were approved by the Ethics Committee of Hebei University of Chinese Medicine (DWLL2018040).

### 2.2 Preparation of BGSD

BGSD consists of Huangqi (Astragali Radix) 15 g, Shanzhuyu (Corni Fructus) 15 g, Mugua (Chaenomelis Fructus) 15 g, Danggui (Angelicae Sinensis Radix) 15 g, Wuweizi (Schisandrae Chinensis Fructus) 15 g, Shanyao (Dioscoreae Rhizoma) 15 g, Chuanxiong (Chuanxiong Rhizoma) 15 g, Baizhu (Atractylodis Macrocephalae Rhizoma) 3 g, Shudihuang (Rehmanniae Radix Praeparata) 3 g, Suanzaoren (Ziziphi Spinosae Semen) 12 g, and Duhuo (Angelicae Pubescentis Radix) 12 g. All Chinese herbs were obtained from Beijing Tongrentang Health Pharmaceutical Co., Ltd. (Shijiazhuang, China), and were prepared following the standardized procedure as described, that is, the Chinese herbal decoction pieces are soaked in deionized water for half an hour, decocted twice, mixed, and concentrated [19]. According to the standard weight of adults (60 kg), the dose for rats was calculated in line with the formula: total weight of BGSD (135 g)/adult weight (60 kg) × conversion coefficient (6.25). A final dosage of 14.06 g/kg was selected for rats.

### 2.3 Models and drug administration

A D-gal-induced aging rat model was established to evaluate the effects of BGSD on learning and memory in

aging rats [20]. After one week of adaption, the rats were allocated to four groups: control, model, BGSD, and piracetam groups ($n$ = 10 in each group). Piracetam group was the positive control group. Rats in the control group were intraperitoneally injected with normal saline [10 mL/(kg·d)], while the rats in other groups were intraperitoneally injected with D-gal [400 mg/(kg·d), dissolved in normal saline, 10 mL/kg; Sigma-Aldrich, USA] for eight weeks to induce aging. Meanwhile, each group was given corresponding drug intervention after modeling, the rats in the BGSD and piracetam groups received gavage of BGSD [14.06 g/(kg·d)] and piracetam [0.4 g/(kg·d), dissolved in normal saline, 10 mL/kg; Huazhong Pharmaceutical Co., Ltd., China] for eight weeks, respectively, while the rats in control and model groups received the same volume of saline [10 mL/(kg·d)].

### 2.4 Observation of the general conditions of the rats

General conditions of the rats, including body weight, food, and water intake, were observed and recorded on days 0, 7, 14, 21, 28, 35, 42, 49, and 56 during the experiment. Food and water intake were calculated based on the formulas: food intake = the previous day's fixed amount – remaining food; water intake = the previous day's fixed amount – remaining water.

### 2.5 Gripping strength test

Place the rat on the grip board, gently grip the back 1/3 of the rat's tail with right hand, and slowly and evenly pull back until the rat releases its claws from the grip board. The gripping strength of rats of each group was measured three times per week, with the mean value as the rat's gripping strength.

### 2.6 Eight-arm maze

The eight-arm maze task was performed following previous research [21, 22]. All rats were fasted 24 h before the test. The experiment lasted for 5 d and the initial two days were the adaptation phase, during which a food pellet was placed at the end of each arm. Next, the rats were placed in the center of the maze, and permitted to travel around to familiarize themselves with the maze for 5 min. Subsequently, in the remaining two days, a food pellet was placed on the four arms (1, 2, 4, and 6), and the rats were trained to enter the baited arms only one time. Rats were assessed on the last day, and the above procedures were repeated. Entering the baited arms only for the first time was considered as a correct choice, whereas re-entrance into a baited arm that had already been visited during the test was referred to as a working memory error (WME). Entrance into unbaited arms was recorded as a reference memory error (RME). The summary of WWE and RME was expressed as the number of total errors (TE).

### 2.7 Step-down test

The step-down test was applied to assess learning and memory [23]. The rats were adapted to the environment for 5 min, then placed on the grid and subjected to electrical stimulation (36 V and 3 mA). The rats immediately jumped on the insulated platform to avoid electric shock, with the training lasting for 5 min. On the second day, the rats were placed on the platform and the grid was electrified for 5 min, and the number of errors in which the rats were subjected to electric shock within 5 min was recorded. Additionally, the step-down latency (the time from the insulated platform onto the grid for the first time) was also recorded.

### 2.8 Sample collection and preparation

Seven rats in each group were randomly selected and were injected with 2% pentobarbital sodium (4 mg/100 g). Subsequently, blood samples were obtained from the femoral artery. Serum samples were obtained by centrifugation (3 500 rpm, 10 min) in sterile EP tubes and stored at – 80 °C for measurement of superoxide dismutase (SOD) and malondialdehyde (MDA) levels. Next, the rats were decapitated and the brains were dissected and weighed. The hippocampus was dissected on ice, divided into three parts, and stored in three sterile EP tubes at – 80 °C for enzyme-linked immunosorbent assay (ELISA), real-time quantitative polymerase chain reaction (RT-qPCR) and Western blot (WB), respectively. Liver, spleen, and thymus tissues were removed from the rats and weighed for organ index calculation. The remaining three rats underwent left ventricular-aortic perfusion and pathological observation of hippocampal tissue was performed. The procedure was as follows: perfused with 0.9% saline and then fixed with 4% paraformaldehyde (PFA). The brains were isolated and post-fixed in 4% PFA (4 °C for 24 h).

### 2.9 Measurement of organ index

The final body weight, brain, liver, spleen, and thymus were weighed, and the organ indices were calculated based on the formula: organ index = organ weight (mg)/the final body weight (g).

### 2.10 Hematoxylin and eosin (HE) staining

The brain tissue was dehydrated with different gradients of ethanol, cleared with xylene, embedded in paraffin, and sliced into 4 μm thickness sections. Subsequently,

the sections were dewaxed in xylene, hydrated with ethanol of different gradients, stained with hematoxylin, differentiated with acid-alcohol solution (a mixture of 1% hydrochloric acid in 70% ethanol), stained with eosin, and dehydrated for HE staining. Finally, the histopathology was observed under a light microscope (BX53, Olympus, Japan).

### 2.11 Measurement of SOD and MDA

The activity of SOD and the level of MDA in serum of the rats were determined following the manufacturer's instructions. The SOD activity was measured using the xanthine oxidase method with an absorbance at 450 nm wavelengths after incubation for 20 min at 37 °C. The MDA levels were assayed by the thiobarbituric acid (TBA) method and the absorbance was detected at 532 nm wavelength.

### 2.12 ELISA

The expression levels of Interleukin (IL)-6, IL-1$\beta$, and tumor necrosis factor (TNF)-$\alpha$ (Thermo Fisher, USA) in the homogenized hippocampus of rats were detected following the instructions of the assay kits.

### 2.13 RT-qPCR

The hippocampus was homogenized and the total mRNA was extracted using a total RNA extraction kit (Promega, USA). RNA was reverse transcribed into first-strand complementary DNA (cDNA) using the GoScript Reverse Transcription System (Promega, USA) based on the protocols of annealing at 25 °C for 5 min, extension at 42 °C for 60 min, and inactivation at 70 °C for 15 min. RT-qPCR amplification was performed using the GoTaq® qPCR Master Mix (Promega, USA) in the following protocol: predenaturation at 95 °C for 10 min followed by 40 cyclic reactions (denaturation: 15 s at 95 °C, annealing: 60 s at 60 °C). The mRNA levels of RAGE, NF-$\kappa$B, IL-1$\beta$, IL-6, and TNF-$\alpha$ were normalized to GAPDH. The RT-qPCR data were analyzed by the comparative threshold cycle (Ct) method, and calculated as RQ = $2^{-\Delta\Delta Ct}$. The primer sequences are listed in Table 1.

### 2.14 WB

The hippocampal tissues were homogenized in Radio Immunoprecipitation Assay (RIPA) lysis buffer [24]. After centrifugation at 8 000 rpm at 4 °C for 10 min, the supernatant of the homogenate was collected. The protein concentration was determined by the bicinchoninic acid (BCA) method (Solarbio, China). An equal amount of protein (50 μg) was separated on a sodium dodecyl sulfate-polyacrylamide gel electrophoresis (SDS-PAGE, 10% gel). The proteins were transferred to a polyvinylidene fluoride membrane for 30 min with 250 mA. The membrane was blocked with 5% nonfat milk for 1 h at room temperature. Subsequently, the membranes were incubated with the following primary antibodies (1 : 1 000, Abcam, UK) against AGEs , RAGE, NF-$\kappa$B, and $\beta$-actin at 4 °C overnight. The membranes were washed thrice with Tris Buffered Saline with Tween (TBST, 10 min each), and incubated with horseradish peroxidase (HRP)-labeled goat anti-rabbit IgG antibody (1 : 10 000, Servicebio Technology Co., Ltd., China) for 1 h. The staining was visualized using the ECL WB Detection Kit (Vazyme, China). The grey intensity was detected by the Image-Pro Plus 6.0 software (IBM, USA).

### 2.15 Statistical analysis

Statistical analyses were performed using the SPSS 23.0 statistical software. One-way analysis of variance (ANOVA) was used to assess group differences for homogeneous and normally distributed data, followed by the Student-Newman-Keuls (SNK) test for pairwise comparisons. The results are presented as mean ± standard deviation (SD). Otherwise, the data were analyzed using the Kruskal-Wallis test. $P < 0.05$ was considered statistically significant.

## 3 Results

### 3.1 Effects of BGSD on body weight, food, and water intake in D-gal-induced aging rats

No significant differences were observed in body weight, food, and water intake among rats in different groups at

**Table 1** Primer sequences used for RT-qPCR

| Gene symbol | Forward primer | Reverse primer |
|---|---|---|
| RAGE | 5'-AGAAACCGGTGATGAAGGACA-3' | 5'-GGTTGTCGTTTTCGCCACAG-3' |
| NF-$\kappa$B | 5'-TGAGTCCCGCCCCTTCTAAA-3' | 5'-CCTGGATCACTTCAATGGCCT-3' |
| IL-6 | 5'-AGCGATGATGCACTGTCAGA-3' | 5'-GGAACTCCAGAAGACCAGAGC-3' |
| IL-1$\beta$ | 5'-GACTTCACCATGGAACCCGT-3' | 5'-GGAGACTGCCCATTCTCGAC-3' |
| TNF-$\alpha$ | 5'-CATCCGTTCTCTACCCAGCC-3' | 5'-AATTCTGAGCCCGGAGTTGG-3' |
| GAPDH | 5'-AGGAAATGATGACCTCCTGAACT-3' | 5'-TGTTTTTGTAAGTATCTTGGTGCCT-3' |

the beginning of the experiment ($P > 0.05$). On the day 21 of modeling, the body weight of rats was significantly decreased in the model group compared with that in the control group ($P < 0.05$). On the day 28 of modeling, the body weight of rats in the BGSD group was significantly increased compared with that in the model group ($P < 0.05$, Figure 1A). And the food intake in the model group was significantly lower than that in the control group ($P < 0.05$). On the day 35 of modeling, the food intake of rats in the BGSD group was significantly higher than that in the model group ($P < 0.05$, Figure 1B). On the day 42 of modeling, the water intake in model group was remarkably reduced compared to that in the control group ($P < 0.05$). On the day 49 of modeling, BGSD treatment significantly reversed the decline in water intake in aging rats ($P < 0.05$, Figure 1C).

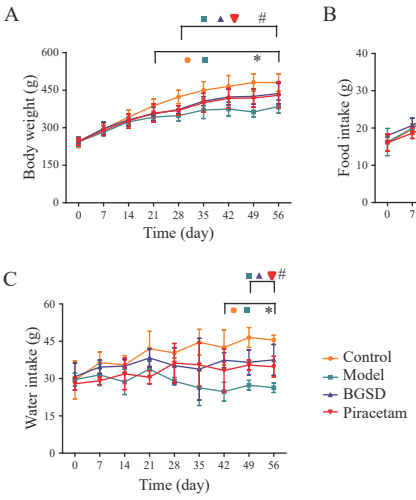


**Figure 1** Body weight, food, and water intake in aging rats

A, body weight. B, food intake. C, water intake. ●: control group. ■: model group. ▲: BGSD group. ▼: piracetam group. *$P < 0.05$, compared with the control group. #$P < 0.05$, compared with the model group.

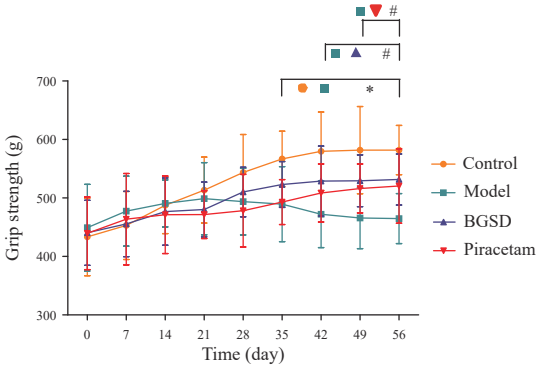


**Figure 2** Gripping strength in aging rats

●: control group. ■: model group. ▲: BGSD group. ▼: piracetam group. *$P < 0.05$, compared with the control group. #$P < 0.05$, compared with the model group.

### 3.2 Effects of BGSD on gripping strength in D-gal-induced aging rats

The gripping strength of rats was illustrated in Figure 2. Rats in the model group appeared significantly decreased gripping strength on the day 35 of modeling compared with the control group at the same time point ($P < 0.05$). Rats in the BGSD group appeared significantly increased gripping strength on the day 42 of modeling compared with the same time point in the model group ($P < 0.05$).

### 3.3 Effects of BGSD on learning and memory impairment in D-gal-induced aging rats

The eight-arm maze task and step-down test were conducted to assess the learning and memory of the rats. The results of the eight-arm maze task indicated that rats in the model group showed a significant increase in WME, RME, and TE compared with those in the control group ($P < 0.05$, Figure 3A - 3C). However, rats in the BGSD group showed a significant decrease in WME, RME, and TE compared with those in the model group ($P < 0.05$). In the step-down test, the number of errors was significantly increased ($P < 0.05$), and the step-down latency was significantly shortened in the model group compared with the control group ($P < 0.05$). By contrast, the number of errors in the BGSD group was significantly decreased ($P < 0.05$), and the step-down latency in the

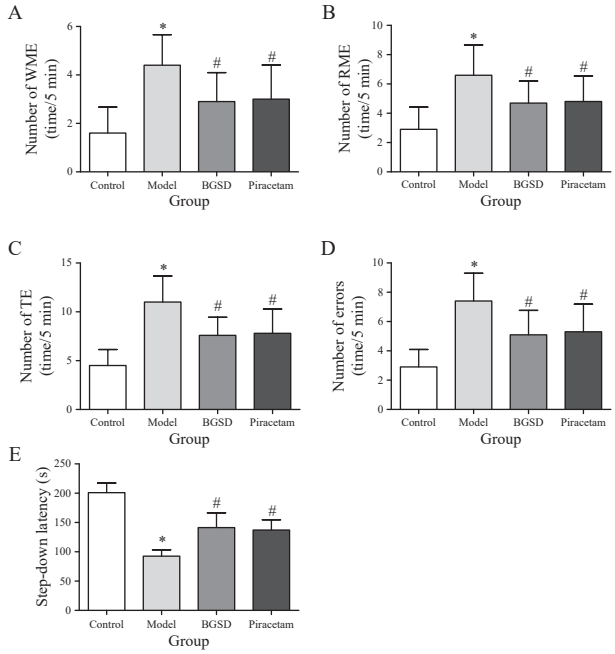


**Figure 3** Learning and memory performance in the eight-arm maze task and step-down test

A, number of WME. B, number of RME. C, number of TE. D, number of errors. E, step-down latency. *$P < 0.05$, compared with the control group. #$P < 0.05$, compared with the model group.

BGSD group was significantly prolonged compared with that in the model group ($P < 0.05$, Figure 3D and 3E). These results demonstrated that BGSD markedly ameliorated the impairment of learning and memory in aging rats.

### 3.4 Effects of BGSD on the brain, liver, spleen, and thymus indexes in D-gal-induced aging rats

The results showed that the indices of brain, liver, spleen, and thymus in the model group were significantly decreased compared with those in the control group ($P < 0.05$, Figure 4). In contrast, the organ indices were significantly ameliorated by BGSD treatment ($P < 0.05$).

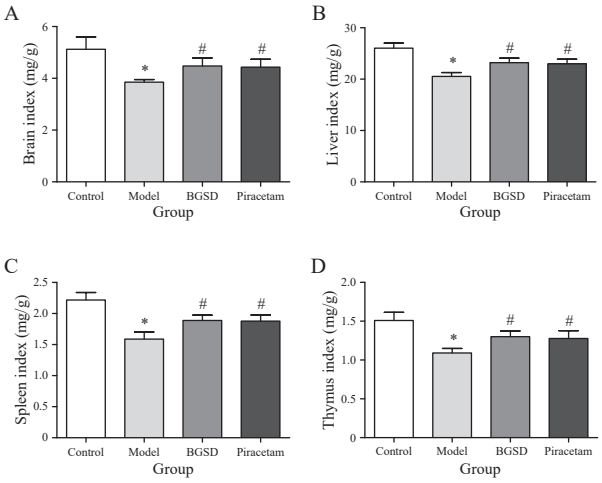


**Figure 4** Indices of brain, liver, spleen, and thymus of rats
A, brain index. B, liver index. C, spleen index. D, thymus index. $^{*}P < 0.05$, compared with the control group. $^{\#}P < 0.05$, compared with the model group.

### 3.5 Effects of BGSD on pathological changes in the hippocampus of D-gal-induced aging rats

HE staining was used to determine the pathological changes in hippocampal tissues (Figure 5). The number of hippocampus neurons was remarkably decreased, the arrangement was disordered, and the cell morphology was irregular in the model group. These pathological changes suggest that the hippocampus of the aging rats displayed noticeable degeneration. By contrast, BGSD treatment markedly alleviated the pathological changes.

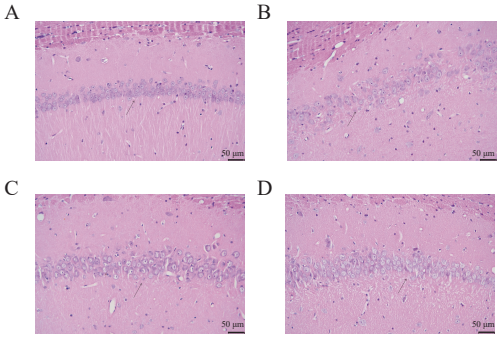


**Figure 5** Pathological changes in the hippocampus CA1 region
A, control group. B, model group. C, BGSD group. D, piracetam group.

### 3.6 Effects of BGSD on the SOD activity and MDA level in serum of D-gal-induced aging rats

Compared with the control group, the SOD activity in the model group was significantly decreased, while the MDA level was significantly increased in the model group ($P < 0.05$, Figure 6). By contrast, BGSD treatment significantly increased the activity of SOD but inhibited the formation of MDA compared with the model group ($P < 0.05$). These data suggested that BGSD could alleviate oxidative damage in aging rats.

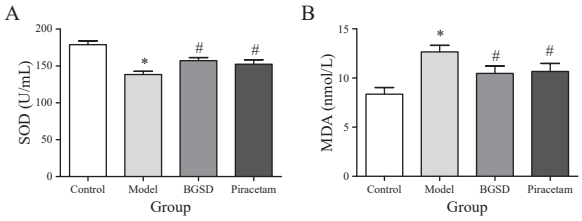


**Figure 6** The SOD activity and MDA level in serum of rats
A, SOD. B, MDA. $^{*}P < 0.05$, compared with the control group. $^{\#}P < 0.05$, compared with the model group.

### 3.7 Effects of BGSD on the levels of IL-6, IL-1$\beta$, and TNF-$\alpha$ in the hippocampus of D-gal-induced aging rats

To verify the changes of inflammation in hippocampal tissues of aging rats, the proinflammatory cytokines IL-6, IL-1$\beta$, and TNF-$\alpha$ were detected by ELISA. Rats in the model group showed significantly higher levels of IL-6, IL-1$\beta$, and TNF-$\alpha$ in the hippocampus than those in the control group ($P < 0.05$, Figure 7). However, BGSD

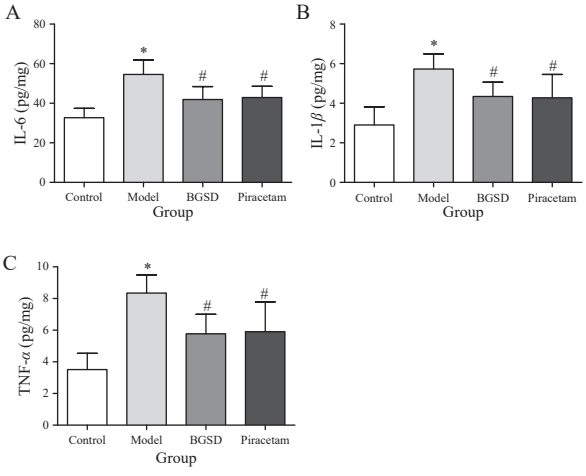


**Figure 7** The levels of pro-inflammatory cytokines in the hippocampus of rats
A, IL-6. B, IL-1$\beta$. C, TNF-$\alpha$. $^{*}P < 0.05$, compared with the control group. $^{\#}P < 0.05$, compared with the model group.

treatment significantly lowered IL-6, IL-1$\beta$, and TNF-$\alpha$ levels in the hippocampus compared with the model group ($P < 0.05$). These results indicated that BGSD down-regulated the expression of proinflammatory factors.

### 3.8 Effects of BGSD on the mRNA expression levels of RAGE, NF-$\kappa$B, IL-6, IL-1$\beta$, and TNF-$\alpha$ in the hippocampus of D-gal-induced aging rats

Compared with the control group, a significant increase was found in the mRNA expression levels of RAGE, NF-$\kappa$B, IL-6, IL-1$\beta$, and TNF-$\alpha$ in the hippocampus in the model group ($P < 0.05$, Figure 8). By contrast, the mRNA expression levels of RAGE, NF-$\kappa$B, IL-6, IL-1$\beta$, and TNF-$\alpha$ in the BGSD group were significantly lower than those in the model group ($P < 0.05$).

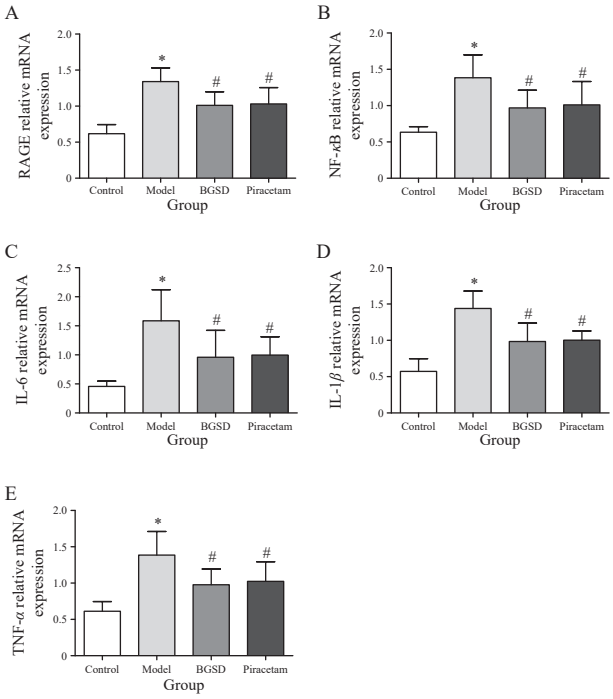


**Figure 8** mRNA expression levels of RAGE, NF-$\kappa$B, IL-6, IL-1$\beta$, and TNF-$\alpha$ in the hippocampus

A - E, the mRNA expression levels of RAGE, NF-$\kappa$B, IL-6, IL-1$\beta$, and TNF-$\alpha$ in four groups, respectively. $^{*}P < 0.05$, compared with the control group. $^{\#}P < 0.05$, compared with the model group.

### 3.9 Effects of BGSD on the protein expression levels of AGEs, RAGE, and NF-$\kappa$B in the hippocampus of D-gal-induced aging rats

Rats in the model group showed higher protein expression levels of hippocampal AGEs, RAGE, and NF-$\kappa$B compared with the control group ($P < 0.05$). By contrast, BGSD treatment down-regulated the expression levels of NF-$\kappa$B, AGEs, and RAGE in the hippocampus compared with the model group ($P < 0.05$, Figure 9).

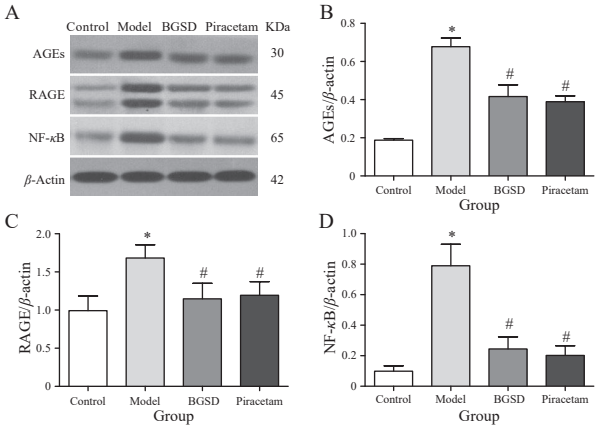


**Figure 9** Protein expression levels of AGEs, RAGE, and NF-$\kappa$B in the hippocampus

A, expressions of AGEs, RAGE, and NF-$\kappa$B by WB analysis. B - D, quantitative evaluation of AGEs, RAGE, and NF-$\kappa$B, respectively. $^{*}P < 0.05$, compared with the control group. $^{\#}P < 0.05$, compared with the model group.

## 4 Discussion

The body system gradually presents a series of degenerative changes during the aging process, especially the structural and functional changes in the brain, resulting in progressive impairment of learning and memory [25]. Therefore, it has become a major public issue and an important challenge to find effective methods to improve aging-related learning and memory impairment. In this study, we found that BGSD improved the behavioral performance in the eight-arm maze task and step-down test, and reversed the pathological changes in the hippocampus. Mechanistically, BGSD possibly exerted the functions by reducing inflammatory reactions and inhibiting the expression of AGEs, RAGE, and NF-$\kappa$B in the hippocampus.

As a reducing sugar, D-gal is commonly found in the body and can be metabolized and absorbed by the body under normal physiological conditions [26]. However, long-term administration of D-gal produces D-galactohexodialdose and hydrogen peroxide under the action of galactose oxidase and galactitol by aldose reductase, causing the imbalance of reactive oxidative stress and activity of antioxidant enzyme, especially MDA level [27]. Thus, the D-gal-induced aging model can mimic the natural aging process [4, 8]. MDA content and SOD activity serve as common biological markers and cornerstones for assessing aging models [28], given the fact that they can indicate the extent of oxidative damage to cells and the body's potential for antioxidant defense. We also found that chronic administration of D-gal promoted MDA level, but reduced SOD activity, which is consistent with previous literature [27]. In addition, aging is accompanied by atrophy of various organs, and the organ index also decreases accordingly. In this study, we detected organ indices. First, the decline of the brain index might be

related to impairment of learning ability. Second, the decline of other organ indices would support the successful establishment of our model. According to the aforementioned findings, the aging model had been successfully established.

Chinese medicine is efficient in treating various diseases with low adverse effects. Based on *Inner Canon of Huangdi* (*Huang Di Nei Jing,*《黄帝内经》), five viscera are important to sustain the normal function of the body and abnormality in the five viscera contribute to aging. *Plain Questions · Treatise on the Six Periods and Visceral Manifestation* (*Suwen · Liujie Zangxiang Lun,*《素问·六节藏象论》) stated: "the liver reflects its brilliance in the nails and fullness in the tendons to produce blood and Qi". The combination of general biological characterization and reduced gripping strength partially confirms the existence of liver Qi deficiency in aging rats. BGSD acts as a representative prescription of supplementing liver Qi. Tonifying liver Qi can delay aging [14]. In the present study, the rats receiving D-gal were characterized by reduced body weight, food and water intake, decreased organ indices of the brain, liver, spleen, and thymus, declined SOD activity, and elevated MDA level. All these symptoms indicated that the aging model was successfully established in rats. In this study, piracetam was selected as the positive control in the treatment of aging and aging-related memory impairment [29]. Similar to piracetam, BGSD not only increased body weight, food intake, water intake, gripping strength, and organ indices of aging rats, but also decreased oxidative damage by reversing the activity of SOD and reducing MDA level. Previous research confirms that the main components of BGSD include Huangqi (Astragali Radix), Shanzhuyu (Corni Fructus), Danggui (Angelicae Sinensis Radix). Huangqi (Astragali Radix) and its active ingredients can provide anti-aging effects [10, 30], which is in line with our study. Meanwhile, Shanzhuyu (Corni Fructus), Danggui (Angelicae Sinensis Radix), and their extracts provide neuroprotection, anti-neuroinflammatory activity, memory improvement, and aging prevention [11-13]. These results indicated that BGSD would be an efficient agent for preventing aging.

Aging is associated with impaired function of multiple organs. Among them, the brain is more vulnerable to impairment, resulting in progressive deterioration of learning and memory function [31]. Moreover, age-related neurodegenerative diseases are related to neuron damage [32]. The eight-arm maze and step-down test are two classical behavioral methods to evaluate learning and memory performance, and are widely used in studies of aging-related learning and memory disorders [33]. Our study suggested that the model group of rats expressed impaired learning and memory behaviors. Conversely, the BGSD group showed better performance in learning and memory. These results demonstrated the potential efficacy of BGSD in ameliorating learning and memory impairment associated with aging in rats.

In addition to the free radical theory, the neuroinflammatory theory has gained attention in the complex mechanism of aging [34]. The decline of learning and memory is closely related to neuroinflammation, and the hippocampus, a well-known region for learning and memory, is more susceptible to damage by inflammatory responses [35]. Trigger factors can stimulate microglia activation, resulting in the release of neurotoxic products, including pro-inflammatory mediators such as IL-6, IL-1$\beta$, and TNF-$\alpha$ to induce chronic neuroinflammation, thereby damaging neurons and causing irreversible neuronal injury, eventually causing progressive decline in learning and memory [36, 37]. Consistently, our results also demonstrated that D-gal-induced aging was associated with the up-regulation of proinflammatory cytokines in the hippocampus. This alter-ration could be reversed by BGSD treatment, suggesting that BGSD could inhibit the secretion of proinflammatory cytokines in the hippocampus.

AGEs are formed by combining the aldehyde group of glucose with the amino group of proteins, nucleic acids, and lipids through a non-enzymatic process called glycation, which plays an important role in degenerative diseases [38, 39]. AGEs accumulate in tissues during aging and damage cell function directly through cytotoxicity [40]. Additionally, AGEs also impair the structure and function of the brain by interacting with its specific receptors to induce neuroinflammation [41]. RAGE is one of the most widely investigated receptors of AGEs, which is a member of the immunoglobulin superfamily. RAGE is widely expressed in microglia, neurons, and endothelial cells [42]. The binding of AGEs with RAGE can activate a variety of signaling pathways, among which the inflammatory response induced by the NF-$\kappa$B pathway was closely related to learning and memory [39]. NF-$\kappa$B is abundant in neurons and micro-glial cells. As a nuclear transcription factor, NF-$\kappa$B can enhance transcription and promote neuroinflammation [43, 44]. The binding of AGEs to RAGE activates the NF-$\kappa$B pathway and triggers the release of pro-inflammatory mediators to induce nerve inflammation, contributing to learning, and memory dysfunction [45]. In this study, the expressions of AGEs, RAGE, and NF-$\kappa$B were prominent in the hippocampus of the aging rats, while BGSD administration suppressed the expression of AGEs, RAGE, and NF-$\kappa$B, indicating that BGSD might mitigate neuroinflammation.

## 5 Conclusion

BGSD demonstrated neuroprotective effects on learning and memory impairment in D-gal-induced aging rats, likely through regulating the AGEs/RAGE/NF-$\kappa$B signaling pathway. BGSD holds potential as an intervention to delay aging and treat age-related diseases.

## Fundings

Scientific Research Project of Hebei Administration of Traditional Chinese Medicine (2020136), and Science Research Project of Hebei Education Department (ZD2022043).

## Competing interests

The authors declare no conflict of interest.

## References

[1] TAI HC, TSAI WK, CHANG ML, et al. Intracavernous injection of platelet-rich plasma reverses erectile dysfunction of chronic cavernous nerve degeneration through reduction of prostate hyperplasia evidence from an aging-induced erectile dysfunction rat model. The FASEB Journal, 2023, 37(4): e22826.

[2] KUO HC, TONG SY, CHAO MW, et al. Ganoderma tsugae prevents cognitive impairment and attenuates oxidative damage in D-galactose-induced aging in the rat brain. PLoS One, 2022, 17(4): e0266331.

[3] LIAN WW, JIA H, XU LJ, et al. Multi-protection of DL0410 in ameliorating cognitive defects in D-galactose induced aging mice. Frontiers in Aging Neuroscience, 2017, 9: 409.

[4] LIU YF, WENG WL, GAO R, et al. New insights for cellular and molecular mechanisms of aging and aging-related diseases: herbal medicine as potential therapeutic approach. Oxidative Medicine and Cellular Longevity, 2019, 2019: 4598167.

[5] ATEF MM, EMAM MN, ABO EL GHEIT RE, et al. Mechanistic insights into ameliorating effect of geraniol on D-galactose induced memory impairment in rats. Neurochemical Research, 2022, 47(6): 1664–1678.

[6] LI L, LI YM, LUO J, et al. Resveratrol, a novel inhibitor of GLUT9, ameliorates liver and kidney injuries in a D-galactose-induced ageing mouse model via the regulation of uric acid metabolism. Food & Function, 2021, 12(18): 8274–8287.

[7] HU Y, FANG X, WANG J, et al. Astragalin attenuates $AlCl_3$/D-galactose-induced aging-like disorders by inhibiting oxidative stress and neuroinflammation. Neurotoxicology, 2022, 91: 60–68.

[8] CHEN B, ZHONG Y, PENG W, et al. Age-related changes in the central auditory system: comparison of D-galactose-induced aging rats and naturally aging rats. Brain Research, 2010, 1344: 43–53.

[9] TAVANAI E, MOHAMMADKHANI G, FARAHANI S, et al. Protective effects of silymarin against age-related hearing loss in an aging rat model. Indian Journal of Otolaryngology and Head & Neck Surgery, 2019, 71(2): 1248–1257.

[10] ZHANG JQ, XUE XL, QIAO YQ, et al. Astragaloside IV extends lifespan of *Caenorhabditis elegans* by improving age-related functional declines and triggering antioxidant responses. Rejuvenation Research, 2021, 24(2): 120–130.

[11] CUI Y, WANG YJ, ZHAO DY, et al. Loganin prevents BV-2 microglia cells from A$\beta$1-42-induced inflammation via regulating TLR4/TRAF6/NF-$\kappa$B axis. Cell Biology International, 2018, 42(12): 1632–1642.

[12] WU YF, WANG XS, SHEN BA, et al. Extraction, structure and bioactivities of the polysaccharides from *Fructus corni*. Recent Patents on Food, Nutrition & Agriculture, 2013, 5(1): 57–61.

[13] ZHU WL, ZHENG JY, CAI WW, et al. Ligustilide improves aging-induced memory deficit by regulating mitochondrial related inflammation in SAMP8 mice. Aging, 2020, 12(4): 3175–3189.

[14] WANG S, LI W, WANG H, et al. Effects of Bugansan on learning and memory function in aging rats based on BDNF/TrkB mediated hippocampal synaptic plasticity. Journal of Beijing University of Traditional Chinese Medicine, 2021, 44(4): 323–331.

[15] WANG JJ, ZHANG TZ, LIU XX, et al. Aqueous extracts of se-enriched *Auricularia auricular* attenuates D-galactose-induced cognitive deficits, oxidative stress and neuroinflammation via suppressing RAGE/MAPK/NF-$\kappa$B pathway. Neuroscience Letters, 2019, 704: 106–111.

[16] LI JS, JI T, SU SL, et al. Mulberry leaves ameliorate diabetes via regulating metabolic profiling and AGEs/RAGE and p38 MAPK/NF-$\kappa$B pathway. Journal of Ethnopharmacology, 2022, 283: 114713.

[17] TÓBON-VELASCO JC, CUEVAS E, TORRES-RAMOS MA. Receptor for AGEs (RAGE) as mediator of NF-$\kappa$B pathway activation in neuroinflammation and oxidative stress. CNS & Neurological Disorders Drug Targets, 2014, 13(9): 1615–1626.

[18] TAN XB, GU JF, ZHAO BJ, et al. Ginseng improves cognitive deficit via the RAGE/NF-$\kappa$B pathway in advanced glycation end product-induced rats. Journal of Ginseng Research, 2015, 39(2): 116–124.

[19] WANG W, ZHANG YX, YU WT, et al. Bushenhuoxue improves cognitive function and activates brain-derived neurotrophic factor-mediated signaling in a rat model of vascular dementia. Journal of Traditional Chinese Medicine, 2020, 40(1): 49–58.

[20] AN L, SUN YC, ZHANG W, et al. Walnut diets up-regulate the decreased hippocampal neurogenesis and age-related cognitive dysfunction in D-galactose induced aged rats. Food & Function, 2018, 9(9): 4755–4762.

[21] KEMSE N, KALE A, CHAVAN-GAUTAM P, et al. Increased intake of vitamin B12, folate, and omega-3 fatty acids to improve cognitive performance in offspring born to rats with induced hypertension during pregnancy. Food & Function, 2018, 9(7): 3872–3883.

[22] HASHIMOTO M, TOZAWA R, KATAKURA M, et al. Protective effects of prescription n-3 fatty acids against impairment of spatial cognitive learning ability in amyloid $\beta$-infused rats. Food & Function, 2011, 2(7): 386–394.

[23] XU C, NIU JJ, ZHOU JF, et al. MicroRNA-96 is responsible for sevoflurane-induced cognitive dysfunction in neonatal rats via inhibiting IGF1R. Brain Research Bulletin, 2019, 144: 140–148.

[24] AHMADI S, KHALEDI S. Anxiety in rats with bile duct ligation is associated with activation of JNK3 mitogen-activated protein kinase in the hippocampus. Metabolic Brain Disease, 2020, 35(4): 579–588.

[25] XIE YR, SONG AN, ZHU YT, et al. Effects and mechanisms of probucol on aging-related hippocampus-dependent cognitive impairment. Biomed & Pharmacother, 2021, 144: 112266.

[26] SUN JZ, ZHANG LH, ZHANG J, et al. Protective effects of ginsenoside Rg1 on splenocytes and thymocytes in an aging rat model induced by D-galactose. International Immunopharmacology, 2018, 58: 94–102.

[27] HADZI-PETRUSHEV N, STOJKOVSKI V, MITROV D, et al. D-galactose induced changes in enzymatic antioxidant status in rats of different ages. Physiological Research, 2015, 64(1): 61–70.

[28] ZHANG C, WEI W, LIU YH, et al. Establishment and evaluation of D-galactose subacute aging rat model. Chinese Journal of Gerontology, 2012, 32(4): 742–745.

[29] LEUNER K, KURZ C, GUIDETTI G, et al. Improved mitochondrial function in brain aging and Alzheimer disease - the new mechanism of action of the old metabolic enhancer piracetam. Frontiers in Neuroscience, 2010, 4: 44.

[30] LIU P, ZHAO HP, LUO YM. Anti-aging implications of Astragalus Membranaceus (Huangqi): a well-known Chinese tonic. Aging and Disease, 2017, 8(6): 868–886.

[31] YAN TX, SHANG L, WANG MS, et al. Lignans from *Schisandra chinensis* ameliorate cognition deficits and attenuate brain oxidative damage induced by D-galactose in rats. Metabolic Brain Disease, 2016, 31(3): 653–661.

[32] SHENG JY, YANG XY, LIU QY, et al. Coadministration with tea polyphenols enhances the neuroprotective effect of defatted walnut meal hydrolysate against scopolamine-induced learning and memory deficits in mice. Journal of Agricultural and Food Chemistry, 2020, 68(3): 751–758.

[33] KIM CH, KO IG, KIM SE, et al. Alpha1-adrenoceptor antagonists improve memory by activating N-methyl-D-aspartate-induced ion currents in the rat hippocampus. International Neurourology Journal, 2015, 19(4): 228–236.

[34] CARDOSO FDS, DE SOUZA OLIVEIRA TAVARES C, ARAUJO BHS, et al. Improved spatial memory and neuroinflammatory profile changes in aged rats submitted to photobiomodulation therapy. Cellular and Molecular Neurobiology, 2022, 42(6): 1875–1886.

[35] WANG YX, CAO XZ, MA H, et al. Prior stressor exposure delays the recovery of surgery-induced cognitive impairment and prolongs neuroinflammation in aged rats. Brain Research, 2016, 1648(Pt A): 380–386.

[36] YAN LC, YANG JH, YU M, et al. Lanthanum impairs learning and memory by activating microglia in the hippocampus of mice. Biological Trace Element Research, 2022, 200(4): 1640–1649.

[37] SHALLIE OF, DALLE E, MABANDLA MV. Memory decline correlates with increased plasma cytokines in amyloid-beta (1-42) rat model of Alzheimer's disease. Neurobiology of Learning and Memory, 2020, 169: 107187.

[38] GUGLIELMOTTO M, ARAGNO M, TAMAGNO E, et al. AGEs/RAGE complex upregulates BACE1 via NF-$\kappa$B pathway activation. Neurobiol Aging, 2012, 33(1): 196.e13–196.e27.

[39] SHI M, YANG S, ZHU XW, et al. The RAGE/STAT5/autophagy axis regulates senescence in mesangial cells. Cellular Signaling, 2019, 62: 109334.

[40] BAYNES JW. The role of AGEs in aging: causation or correlation. Experimental Gerontology, 2001, 36(9): 1527–1537.

[41] HONG Y, SHEN C, YIN QQ, et al. Effects of RAGE-specific inhibitor FPS-ZM1 on amyloid-beta metabolism and AGEs-induced inflammation and oxidative stress in rat hippocampus. Neurochemical Research, 2016, 41(5): 1192–1199.

[42] YIN QQ, DONG CF, DONG SQ, et al. AGEs induce cell death via oxidative and endoplasmic reticulum stresses in both human SH-$SY_5Y$ neuroblastoma cells and rat cortical neurons. Cellular and Molecular Neurobiology, 2012, 32(8): 1299–1309.

[43] SONG CM, ZHANG YS, CHENG L, et al. Tea polyphenols ameliorates memory decline in aging model rats by inhibiting brain TLR4/NF-$\kappa$B inflammatory signaling pathway caused by intestinal flora dysbiosis. Experimental Gerontology, 2021, 153: 111476.

[44] ZHAO YC, LIU XL, ZHENG YN, et al. Aronia melanocarpa polysaccharide ameliorates inflammation and aging in mice by modulating the AMPK/SIRT1/NF-$\kappa$B signaling pathway and gut microbiota. Scientific Reports, 2021, 11(1): 20558.

[45] LI W, WANG S, WANG H, et al. Astragaloside IV prevents memory impairment in D-galactose-induced aging rats via the AGEs/RAGE/NF-$\kappa$B axis. Archives of Medical Research, 2022, 53(1): 20–28.

# 基于 AGEs/RAGE/NF-κB 通路探讨补肝散改善 D-半乳糖致衰大鼠学习记忆障碍机制研究

李伟[a], 王硕[a], 王杰鹏[a, b], 方芳[a, b], 方朝义[a, b*]

*a. 河北中医药大学基础医学院, 河北 石家庄 050200, 中国*
*b. 河北省中西医结合肺病研究重点实验室, 河北 石家庄 050091, 中国*

**【摘要】目的** 探讨复方补肝散（BGSD）干预 D-半乳糖致衰大鼠学习记忆能力的潜在作用机制。**方法** 40 只大鼠被随机分为对照组、模型组、BGSD［14.06 g/(kg·d)］组和吡拉西坦［0.4 g/(kg·d)］组，每组 10 只。腹腔注射 D-半乳糖［400 mg/(kg·d)］建立衰老大鼠模型。每周记录大鼠体质量、摄水量、摄食量和抓力；八臂迷宫和跳台实验评估大鼠学习记忆能力；称取肝脏、胸腺、脾脏和脑组织重量以计算相应脏器指数；检测血清丙二醛（MDA）含量和超氧化物歧化酶（SOD）活性；苏木精-伊红（HE）染色观察海马病理学改变；酶联免疫吸附法（ELISA）检测海马肿瘤坏死因子-α（TNF-α）、白细胞介素（IL）-6 及 IL-1β 水平；实时荧光定量 PCR（RT-qPCR）检测海马晚期糖基化终末产物受体（RAGE）、核因子-κB（NF-κB）、TNF-α、IL-6 和 IL-1β mRNA 表达；蛋白免疫印迹法（WB）检测海马晚期糖基化终末产物（AGEs）、RAGE 和 NF-κB 蛋白表达。**结果** 补肝散可显著增加 D-半乳糖致衰大鼠的摄食量、摄水量、体质量、抓力及脏器指数（$P < 0.05$），减少八臂迷宫中工作记忆错误（WME）、参考记忆错误（RME）以及总记忆错误次数（TE）（$P < 0.05$），降低跳台实验中错误次数并延长跳台潜伏期（$P < 0.05$）。此外，补肝散可减少海马神经元损伤，提高血清 SOD 活性，降低 MDA 含量及下调促炎因子 TNF-α、IL-6 和 IL-1β 水平（$P < 0.05$）。进一步研究结果显示，补肝散可显著降低海马 AGEs、RAGE 和 NF-κB 表达（$P < 0.05$）。**结论** 补肝散可通过抑制 AGEs/RAGE/NF-κB 信号通路调节 D-半乳糖致衰大鼠神经炎症损伤从而改善学习记忆能力。

**【关键词】**补肝散；肝气虚；衰老；学习记忆；神经炎症；AGEs/RAGE/NF-κB 信号通路